Inhibition of the Bacterial Enoyl Reductase FabI by Triclosan: A Structure−Reactivity Analysis of FabI Inhibition by Triclosan Analogues†

Sharada Sivaraman,§ Todd J. Sullivan,§ Francis Johnson,§,# Polina Novichenok,§ Guanglei Cui,§ Carlos Simmerling,§ and Peter J. Tonge*,§

Department of Chemistry, SUNY at Stony Brook, Stony Brook, New York 11794-3400, and Department of Pharmacological Sciences, SUNY at Stony Brook, Stony Brook, New York 11794-8651

Received April 17, 2003

To explore the molecular basis for the picomolar affinity of triclosan for FabI, the enoyl reductase enzyme from the type II fatty acid biosynthesis pathway in *Escherichia coli*, an SAR study has been conducted using a series of triclosan analogues. Triclosan (**1**) is a slow, tight-binding inhibitor of FabI, interacting specifically with the E·NAD^+ form of the enzyme with a K_1 value of 7 pM. In contrast, 2-phenoxyphenol (**2**) binds with equal affinity to the E·NAD^+ ($K_1 = 0.5$ μM) and E·NADH ($K_2 = 0.4$ μM) forms of the enzyme and lacks the slow-binding step observed for triclosan. Thus, removal of the three triclosan chlorine atoms reduces the affinity of the inhibitor for FabI by 70 000-fold and removes the preference for the E·NAD^+ FabI complex. 5-Chloro-2-phenoxyphenol (**3**) is a slow, tight-binding inhibitor of FabI and binds to the E·NAD^+ form of the enzyme ($K_1 = 1.1$ pM) 7-fold more tightly than triclosan. Thus, while the two ring B chlorine atoms are not required for FabI inhibition, replacement of the ring A chlorine increases binding affinity by 450 000-fold. Given this remarkable observation, the SAR study was extended to the 5-fluoro-2-phenoxyphenol (**4**) and 5-methyl-2-phenoxyphenol (**5**) analogues to further explore the role of the ring A substituent. While both **4** and **5** are slow, tight-binding inhibitors, they bind substantially less tightly to FabI than triclosan. Compound **4** binds to both E·NAD^+ and E·NADH forms of the enzyme with K_1 and K_2 values of 3.2 and 240 nM, respectively, whereas compound **5** binds exclusively to the E·NADH enzyme complex with a K_2 value of 7.2 nM. Thus, the ring A substituent is absolutely required for slow, tight-binding inhibition. In addition, pK_a measurements coupled with simple electrostatic calculations suggest that the interaction of the ring A substituent with F203 is a major factor in governing the affinity of analogues **3**−**5** for the FabI complex containing the oxidized form of the cofactor.

Introduction

The pathway for fatty acid biosynthesis (FAS) in *Escherichia coli* is a paradigm for understanding type II FAS systems in other bacteria and has been extensively studied. The differences in protein sequences and active site organization between the human and bacterial FAS systems make it possible for specific inhibitors to be designed against the bacterial FAS enzymes, and thus this system has been validated as an excellent drug target for the design of antimicrobial agents.[1−3]

FabI, the NADH-dependent *trans*-2-enoyl-ACP reductase (ENR) in *E. coli*, is the key regulator of fatty acid biosynthesis. ENRs have been shown to be inhibited by diazaborines, isoniazid, triclosan, and more recently by other new classes of novel inhibitors.[4−7] Triclosan (Scheme 1) (5-chloro-2-(2,4-dichloro-phenoxy)-phenol) is a broad-spectrum biocide that has been in use for over 30 years, mainly as a component of antimicrobial wash products in health-care settings. More recently, triclosan has found extensive use in consumer products such as toothpaste, mouthwashes, deodorants, hand soaps, and lotions. It is also incorporated in children's toys, cutting boards, and the plastic film used to wrap meat products.[8] Until recently, it was thought that triclosan, being a small hydrophobic molecule, was absorbed via diffusion into the bacterial cell wall and that nonspecific disruption of the cell wall was the mechanism by which triclosan exhibited its antibacterial

Scheme 1

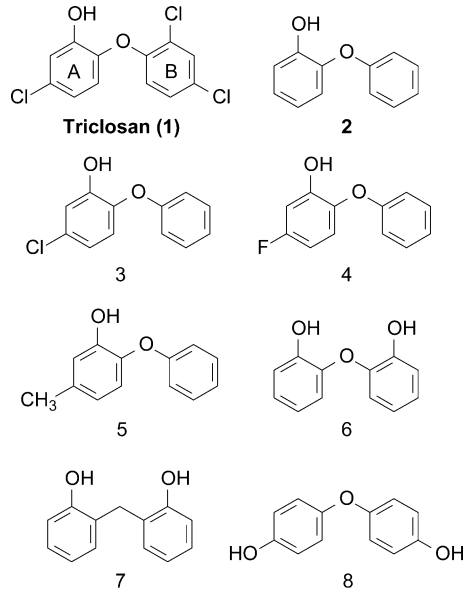

† This work was supported by NIH Grant AI44639 to P.J.T. P.J.T. is an Alfred P. Sloan Research Fellow.

* To whom correspondence should be addressed. Telephone: (631) 632 7907. Fax: (631) 632 7960. E-mail: peter.tonge@sunysb.edu.
§ Department of Chemistry.
# Department of Pharmacological Sciences.

10.1021/jm030182i CCC: $27.50
Published on Web 01/06/2004

activity[9,10] However, the first evidence that triclosan inhibits fatty acid biosynthesis came when a strain of *E. coli* resistant to triclosan was isolated, and the resistance was mapped to the *fabI* gene which codes for the *E. coli* ENR.[11] Subsequently, extensive biochemical and structural studies have been performed to substantiate triclosan as a specific *E. coli* FabI inhibitor.[12−16] Two ENR isoforms, FabK and FabL, have been discovered in the gram-positive bacteria, *Streptococcus pneumoniae* and *Bacillus subtillis*, respectively.[17,18] FabK is resistant to triclosan, whereas FabL is reversibly inhibited by triclosan. Triclosan also directly inhibits the FabI from *Staphylococcus aureus*,[19] *Haemophilus influenzae*,[20] the ENR from *Mycobacterium tuberculosis*, InhA,[21−23] and the ENR from *Plasmodium falciparum*, the malarial parasite.[24−26] A recent report also suggests that triclosan inhibits enoyl reductase of type I fatty acid synthase and may be a potential candidate for breast cancer chemotherapy.[27]

The common theme in the inhibition of ENRs by triclosan is the requirement of the NAD^+ cofactor. In most cases, triclosan forms a stable ternary complex with the enzyme−cofactor complex as shown by several X-ray structures of the FabI−NAD^+−triclosan complex.[14,15,23,26,28,29] Unlike the diazaborines and isoniazid, triclosan does not form a covalent adduct with the bound NAD^+ cofactor. The interaction of triclosan with FabI is stabilized by the $\pi-\pi$ stacking interaction between the hydroxychlorophenyl ring (ring A) and the nicotinamide ring of the NAD cofactor. The 2′-hydroxyl group of the NAD^+ ribose ring and the hydroxyl group of Y156 form hydrogen bonding interactions with the hydroxyl group of triclosan. Ring B makes several hydrophobic contacts with FabI. The ether oxygen of triclosan may also be critical in the formation of the stable FabI−triclosan−NAD^+ complex, since the replacement of this group by a sulfur atom abolishes inhibitory activity.[12] A diphenylamine triclosan analogue, which carries nitrogen as the bridging atom, has been shown to adopt a similar conformation when bound to the malarial ENR.[26] Most of the features unique to triclosan binding to FabI are preserved in this structure, thus revealing the importance of these interactions. Furthermore, X-ray crystal structure data from the two new and chemically distinct classes of FabI inhibitors bound to FabI in the presence of NAD^+ corroborate the common themes in the binding of ENR inhibitors to FabI.[4,5]

The key feature of the inhibition of the *E. coli* FabI by triclosan is the slow, tight-binding step, which has been determined by detailed kinetic analysis.[13,30] Unlike classical inhibitors, that act almost instantaneously, slow-binding inhibitors take several minutes, hours, or even days for their inhibitory effects to take place. The longer life of the EI complex in vivo makes them very potent drug candidates.[31] The slow onset of tight-binding inhibition likely arises from a conformational change that occurs following formation of the initial FabI−triclosan complex. Although no direct evidence has been obtained for this change, the only structural perturbation that has been seen so far is the ordering of the substrate binding loop upon triclosan binding. Interestingly, the crystal structures of the *E. coli* FabI with NAD^+ and diazaborine compounds reveal a similar ordering of the loop.[32,33] Recently, in a structure−reactivity study of diazaborine inhibition of the *E. coli* FabI, Rafferty and co-workers have shown that the loop adopts two distinct conformations for separate monomers of the FabI−NAD^+−diazaborine complex. The reordering of the loop brings certain amino acids closer to the fused rings of the inhibitor and introduces newer contacts with the cofactor. Similar observations have been made by examining the A138G mutant *B. napus* plant ENR−NAD^+−thienodiazaborine crystal structure.[34] All the above data suggest that the flexibility of the loop (residues 192−198) plays an important role in inhibitor binding and substrate recognition.

Scheme 2

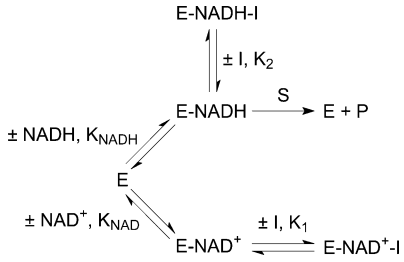

The antibacterial activity of several 2-hydroxydiphenyl ethers as well as hexachlorophene and 2-hydroxydiphenylmethanes have been determined.[12,19,26] These studies have revealed the importance of the hydroxyl group and the bridging oxygen in triclosan inhibition of the *E. coli* FabI. We recently reported a detailed kinetic analysis of the triclosan inhibition of triclosan-resistant and active-site mutant FabIs. We observed that FabI mutations alter the relative affinity of triclosan for the E·NADH and E·NAD^+ forms of the enzyme, suggesting that the oxidation state of the cofactor, as well as the electron density of triclosan, play an important role in the inhibition of FabI by triclosan.[30] Here we investigate the SAR for triclosan inhibition of FabI to gain a better understanding of the contributions of the enzyme−triclosan interactions that lead to potent inhibition of this enzyme. We have made stepwise changes in the triclosan structure (Scheme 1) and probed the effect of these changes on the ability of the inhibitor to bind to the wild-type enzyme. The present SAR analysis combined with the studies on mutant FabIs together with X-ray structural data provides important information about the molecular basis of triclosan inhibition.

Results

Data Analysis for Slow, Tight-Binding Inhibition of FabI: Revisiting the Inhibition of Wild-Type FabI by Triclosan. The method used to quantitate the slow, tight-binding inhibition of FabI by triclosan is based on the procedure developed by Ward et al.[13] In the present study, we have modified the data analysis described by Ward et al. and used by us in a previous publication. The principal differences between the present approach and that used previously are (i) our equations describe the general case for Scheme 2 and so separate equations need not be used depending on which cofactor is varied and (ii) no correction factors are required for the values of K_1 or K_2 obtained from data fitting. When eq 2 is used to fit data for triclosan binding to wild-type enzyme, values of 7 ± 1 pM and >1 M are obtained for K_1 and K_2, respectively, consistent

Table 1. Data for Triclosan Analogues: pK_a, Minimum Inhibitory Constants Toward *E. coli*, and Inhibition Constants for Binding to Wild-Type FabI

			FabI inhibition		
compound	pK_a	MIC *E. coli* (μg/mL)[a]	K_1	K_2	binding preference
triclosan (**1**)	7.8 ± 0.1 8.4 ± 0.1[b]	0.3	7 ± 1 pM[c]		E·NAD$^+$ [d]
2	9.12 ± 0.03	3.7	0.50 ± 0.02 μM	0.40 ± 0.01 μM	NC with respect to DDCoA[e]
3	8.13 ± 0.02	0.07	1.1 ± 0.1 pM		E·NAD$^+$ [d]
4	8.12 ± 0.06	0.6	3.2 ± 0.4 nM	42 ± 1 nM	E·NAD$^+$ and E·NADH[d]
			68 ± 8 pM	240 ± 40 nM	E·NAD$^+$ and E·NADH[d]
5	9.15 ± 0.09	1.0		7.2 ± 0.2 nM	E·NADH[d]
				9.7 ± 0.4 nM	E·NADH[d]
6	ND[f]	2.0	0.15 ± 0.01 μM		UC with respect to DDCoA[g]
7	ND[f]	>40	53 ± 8 μM	30 ± 5 μM	NC with respect to DDCoA[e]
8	ND[f]	>100	1.7 mM	1.9 mM	NC with respect to DDCoA[e]

[a] The experiment was repeated twice for each analogue and the values reported are average of two readings. [b] pK_a for triclosan bound to FabI.[30] [c] Data from Sivaraman et al.[30] [d] Slow binding inhibition. [e] Noncompetitive inhibition. K_{ii} and K_{is} have been listed under K_1 and K_2, respectively. [f] ND: not determined. [g] Uncompetitive inhibition. K_{ii} has been listed under K_1.

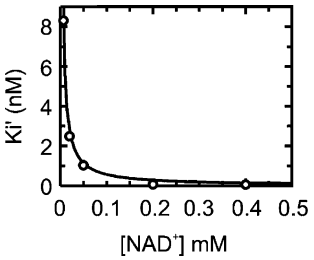

Figure 1. The effect of NAD$^+$ on the apparent inhibition constant for **3** binding to wild-type FabI. The data have been fitted to eq 3 with $K_1 = 1.1 \pm 0.1$ pM.

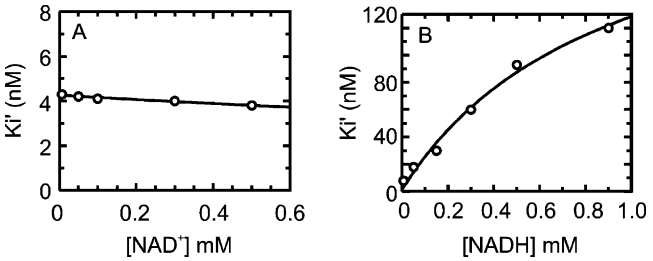

Figure 2. Triclosan analogue **4** inhibition of FabI. (A) The effect of NAD$^+$ on the apparent inhibition constant. The data have been fitted to eq 2 to give $K_1 = 3.2 \pm 0.4$ nM and $K_2 = 42 \pm 1$ nM. (B) The effect of NADH on the apparent inhibition constant for binding of **4** to FabI. The data have been fitted to eq 2 to give $K_1 = 68 \pm 8$ pM and $K_2 = 240 \pm 40$ nM.

with the knowledge that triclosan binds exclusively to the E·NAD$^+$ complex. In agreement with this expectation, subsequent reanalysis of these data using eq 3 provided a K_1 value of 7 ± 1 pM. This new value of K_1 is approximately 3-fold smaller than the value of 23 ± 1 pM determined previously,[30] and results from the use of $K_{dNADH} = 5.6$ μM[13] in place of $K_{mNADH} = 20$ μM[30] to estimate the fraction of enzyme present as the E·NADH complex in the incubation mixtures prior to the addition of DDCoA. Since the preincubations of enzyme, cofactor, and inhibitor are performed in the absence of the enoyl-CoA substrate, K_{dNADH} must be used rather than K_{mNADH}. We note that this does not affect Ward's analysis in which crotonyl-CoA was used as the substrate since $K_{dNADH} = K_{mNADH} = 5.6$ μM.[13]

Inhibition of Wild-Type FabI by Triclosan Analogues 3−5. Table 1 lists the inhibition constants obtained for triclosan analogues binding to the wild-type FabI enzyme. Analogues **3**−**5** are all slow-binding inhibitors of the enzyme. Equation 2 was used to fit the data for analogue **3** obtained when [NAD$^+$] was varied at saturating [NADH] giving a K_1 value of 1.1 ± 0.1 pM and $K_2 > 1$ M. Reanalysis of these data using eq 3 provided a K_1 value of 1.1 ± 0.1 pM (Figure 1). Consequently, analogue **3** binds preferentially to the E·NAD$^+$ form of the enzyme with an affinity that is around 7-fold higher than that seen for triclosan (K_1 = 7 pM).

For analogue **4**, K_i' decreased slightly as [NAD$^+$] increased (Figure 2A) suggesting that this analogue bound to both E·NAD$^+$ and E·NADH with a preference for E·NAD$^+$. Data fitting using eq 2 when [NAD$^+$] was varied at a constant [NADH] gave K_1 and K_2 values of 3.2 ± 0.4 and 42 ± 1 nM, respectively (Figure 2A). To confirm that analogue **4** had a preference for the E·NAD$^+$ form of FabI, the experiment was repeated varying [NADH], while keeping [NAD$^+$] constant. In Figure 2B, it can be seen that the observed K_i' values increased as a function of [NADH], again consistent with a model in which the analogue is bound to both cofactor-bound forms of the enzyme with a preference for E·NAD$^+$. When these data were analyzed using eq 2, values of 68 ± 8 pM and 240 ± 40 nM were obtained for K_1 and K_2, respectively.

The value of K_1 obtained in the varied NADH experiment with analogue **4** is significantly smaller (50-fold) than K_1 determined in the varied NAD$^+$ experiment, while there is a 6-fold difference in the K_2 values between the two experiments. Although the use of eq 2 enables both K_1 and K_2 to be extracted from a single experiment, it is likely that greater reliability can be attached to the dissociation constant describing inhibitor binding to the form of the enzyme for which the cofactor was being varied. In the varied NAD$^+$ experiment, this is K_1 (3.2 nM), while in the varied NADH experiment this is K_2 (240 nM). In addition, since the experimental design was established to quantitate the binding of triclosan to FabI where the interaction is exclusively with E·NAD$^+$, [NADH] in the varied NAD$^+$ experiment is present at a much greater concentration than its K_d, while [NAD$^+$] in the varied NADH experiment is present at a much lower concentration than its K_d. Thus, one possible explanation for the variation in K_1 and K_2 between the experiments with analogue **4** concerns the experimental precision of the dissociation constants calculated in each experiment. However, a second explanation is that the analogue is also binding

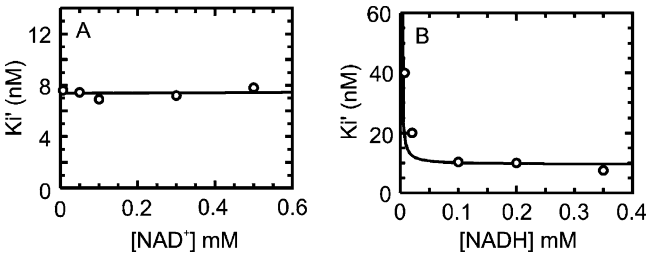

Figure 3. Triclosan analogue **5** inhibition of FabI. (A) The effect of NAD^+ on the apparent inhibition constant. The data have been fitted to eq 4 to give with $K_2 = 7.2 \pm 0.2$ nM. (B) The effect of NADH on the apparent inhibition constant for binding of **5** to FabI. The data have been fitted to eq 4 to give $K_2 = 9.7 \pm 0.4$ nM.

to the free enzyme so that an E·I inhibited complex is present in addition to the E·NADH·I and E·NAD^+·I complexes. To account for the presence of E·I in the data analysis, an additional term $1/K_3$ must be added to the two terms in the denominator to eq 2, where K_3 is the dissociation constant of the analogue for free enzyme. Iterative fitting of the data provided estimates of $K_1 = 3.2 \pm 0.3$, $K_2 = 100 \pm 400$, and $K_3 = 2 \pm 4$ nM when [NAD^+] was varied and $K_1 = 6 \pm 4000$, $K_2 = 240 \pm 50$, and $K_3 = 1.5 \pm 0.2$ nM when [NADH] was varied. Thus, while K_1 in the varied NAD experiment and K_2 in the varied NADH experiment have similar, well-defined values to those determined by eq 2 above, the inclusion of a term to account for binding of analogue **4** to free enzyme with a dissociation constant of 1−2 nM has improved the agreement between these values and K_2 in the varied NAD^+ experiment and K_1 when NADH was varied, but with a substantial loss of precision. The observation that inclusion of K_3 substantially increases the error in K_1 and K_2 therefore argues against the possibility that the inhibitor might also bind to the free enzyme.

Inhibition by analogue **5** showed exclusive binding preference to E·NADH as seen by the data which fit well with eq 4 yielding a K_2 value of 7.2 ± 0.2 nM (Figure 3A). The selectivity of analogue **5** for binding to E·NADH was verified in experiments in which NADH was varied and a K_2 value of 9.7 ± 0.4 nM was obtained (Figure 3B).

Inhibition of Wild-Type FabI by Triclosan Analogues 2 and 6−8. In contrast to analogues **3**−**5**, analogue **2**, which is the triclosan analogue without any chlorine atoms, is a classical reversible inhibitor of the wild-type enzyme. Plots of v versus v/[DDCoA] gave parallel lines (data not shown), indicating noncompetitive inhibition of FabI by **2**, and data fitting using eq 5 gave K_{is} and K_{ii} values of 0.5 and 0.4 μM, respectively. On the basis of our knowledge of how triclosan binds to FabI and the related enzyme from *M. tuberculosis*,[13,22,28,30] we assign K_{ii} to the dissociation constant for binding to the E·NAD^+ complex and K_{is} to the dissociation constant for binding to E·NADH. Thus, removal of all three triclosan chlorine atoms has reduced the affinity of the enzyme for the inhibitor by over 70 000-fold and removed the preference for the E·NAD^+ complex. Analogues **6**−**8** were also classical reversible inhibitors of wild-type FabI. Plots of v versus v/[DDCoA] for each concentration of analogue **6** intersected on the x-axis, indicating uncompetitive inhibition with respect to DDCoA with $K_{ii} = 0.15$ μM (data not shown). In the case of analogues **7** and **8**, the plots of v versus v/[DDCoA] gave parallel lines indicating noncompetitive inhibition with K_{ii} and K_{is} values of 53 and 30 μM, respectively, for analogue **7** and 1.7 and 1.9 mM, respectively, for analogue **8** (data not shown).

Table 2. Calculated Interaction Energies[a] between the Triclosan Analogues and NAD^+

compound	calculated interaction energy kcal/mol	experimental binding energy for E·NAD^+[b]
triclosan (**1**)	−18.19	−15.46
2	−15.77	−8.73
3	−17.32	−16.56
4	−16.69	−11.76
5	−16.35	−7.20[c]

[a] Interaction energies between the triclosan analogues and NAD^+ were calculated with a molecular mechanics approach using the AMBER 7 modeling package and the parm99 force field. [b] Calculated from K_1 in Table 1. [c] Since binding to E·NAD^+ is not observed for analogue **5**, it was assumed that K_1 is at least 100-fold larger than K_2.

Determination of pK_a Values for Triclosan and Analogues 2−5. Table 1 gives the pK_a values determined for triclosan and analogues **2**−**5**. The pK_a of 7.8 for triclosan matches well with the pK_a value reported for this compound in the literature.[13] When bound to FabI, the pK_a for triclosan is increased to 8.4. Compound **2**, which is the triclosan analogue without chlorines, has a pK_a of 9.12 which is 1.3 units higher than triclosan. Compounds **3** and **4** have identical pK_a values of 8.13 and 8.12, which are each a unit lower than that of **2** and consistent with the inductively electron withdrawing effect of the meta substitution with respect to the hydroxyl group of **2**. Analogue **5**, which has a methyl group meta to the hydroxyl group, has a higher pK_a value of 9.15.

Calculated Interaction Energies Between Each Analogue and NAD^+. The interaction between triclosan analogues and NAD^+ was calculated with a molecular mechanics approach using the AMBER 7 modeling package and the parm99 force field. The results of these calculations are given in Table 2. Triclosan gave the most favorable interaction energy with a value of −18.19 kcal/mol, while analogue **2**, in which all the chlorine atoms have been removed, gave the least favorable interaction energy with a value of −15.77 kcal/mol.

Determination of Whole Cell Antimicrobial Activity. Table 1 gives the MIC values for triclosan and analogues **2**−**8**. They range from 0.07 to 100 μg/mL.

Discussion

Triclosan and 2-Phenoxyphenol (2). Triclosan is a slow, tight-binding picomolar inhibitor of the wild-type *E. coli* FabI ($K_1 = 7$ pM) and binds preferentially to the E·NAD^+ form of the enzyme. To investigate the molecular basis for the high affinity of triclosan for FabI, we have performed a structure−activity analysis by making systematic changes to the triclosan diphenyl ether skeleton and examining the impact of these changes on enzyme inhibition. Inspection of the FabI−NAD^+−triclosan crystal structure reveals several potentially important interactions between the inhibitor and the enzyme including hydrogen bonds between the ring A hydroxyl and the hydroxyl groups of Y156 (2.7

Å) as well as the ribose sugar of NAD^+ (2.60 Å), an interaction between F203 and the ring A chlorine and a stacking interaction between ring A and the nicotinamide ring of NAD^+.[15] The importance of the interactions involving Y156 and F203 have previously been examined by analyzing the inhibition of the Y156F and F203L mutants by triclosan. For both mutants, triclosan binds to both the E·NAD^+ and E·NADH forms of FabI, albeit with a continued preference for E·NAD^+, and affinity of the inhibitor for the enzyme is reduced 100- (F203L) to 400- (Y156F) fold.[30] The data for Y156F are consistent with other studies in which it has been shown that removal of the triclosan ring A hydroxyl decreases affinity by more than 10 000-fold.[13]

We initiated our SAR study by examining the binding of analogue **2**, which lacks the three triclosan chlorine atoms. Significantly, analogue **2** binds 70 000-fold less tightly to FabI than does triclosan. In addition, unlike triclosan, analogue **2** is not a slow-binding inhibitor and also binds to both the E·NAD^+ and E·NADH forms of FabI. Thus, removal of all three chlorine atoms from triclosan has substantially reduced the affinity of the inhibitor for the enzyme and also removed the preference for the E·NAD^+ enzyme complex. It has been proposed that the structure of the enolate anion intermediate of the substrate is closely mimicked by the phenolic ring of triclosan, leading to the proposal that triclosan would be bound as the anion to FabI.[14] Consequently, the decrease in affinity observed for analogue **2** compared to triclosan could in part be due to an alteration in the ionization state of the bound analogue since the pK_a values for **2** and triclosan are 9.12 and 7.8, respectively (Table 1). However, we determined the pK_a of triclosan bound to FabI and observed that the triclosan pK_a increases from 7.8 for free inhibitor to 8.4 when bound to the enzyme. Thus, triclosan is bound to FabI as the neutral species rather than the anion. Since the free pK_a of **2** is more basic than triclosan, we expect analogue **2** to also be bound as the neutral species to FabI. Thus, the decrease in affinity observed for **2** compared to triclosan likely does not result from an alteration in the ionization state of the analogue. Alteration of the phenolic hydroxyl pK_a value could alter the strength of hydrogen bonding interactions involving this group, however this effect is likely to be small compared to the 70 000-fold decrease in affinity of **2** relative to triclosan.

5-Chloro-2-Phenoxyphenol (3). To understand the relative importance of the chlorine atoms, we next examined analogue **3** which has a chlorine atom at the 5-position meta with respect to the hydroxyl group on ring A. We predicted that the inhibition constant for the binding of **3** to FabI would be the ultimate test for the contribution of ring A to inhibition since it is the same as in the triclosan structure. In addition, since ring B points away from the active site and makes few hydrophobic contacts with the protein,[15] this analogue would enable us to evaluate the contribution of ring B toward binding. Analogue **3** is a slow, tight-binding inhibitor of the enzyme, binding preferentially to E·NAD^+ with a K_1 value of 1.1 pM. Remarkably, restoring the chlorine atom to ring A increases the affinity 450 000-fold. As noted above, the ring A chlorine forms an edge-on π interaction with the aromatic ring of F203 while replacement of this residue with Leu results in a 100-fold decrease in affinity.[15,30] Consequently, the interaction of the ring A chlorine with F203 is pivotal in controlling the affinity of the analogue for the enzyme.

The observation that the deletion of the two chlorine atoms on ring B increases the affinity 7-fold is significant and suggests that the ring B chlorine atoms participate in unfavorable steric interactions with the enzyme. Consistent with this observation, the MIC value for analogue **3** (0.07 μg/mL) is around 4-fold lower than that of triclosan (0.3 μg/mL), supporting the contention that the antibacterial activity of triclosan results primarily from an inhibition of FabI. To probe the role of ring B further, we studied the inhibition of the enzyme by 3-chloro-benzene-1, 2-diol, a triclosan analogue which has a hydroxyl group in the place of ring B. While we did not complete a full kinetic analysis for 3-chloro-benzene-1,2-diol, we observed that at 180 μM only 25% of the enzyme activity was inhibited (data not shown). Thus, the replacement of ring B by a hydroxyl group decreases affinity by more than 10^6-fold. Consistent with this large decrease in affinity for FabI, 3-chloro-benzene-1,2-diol had no effect on cell growth up to a concentration of 100 μg/mL. These SAR data indicate that whereas the ring B chlorine atoms are not important for enzyme inhibition or biological activity, ring B itself must be retained.

5-Fluoro-2-Phenoxyphenol (4) and 5-Methyl-2-Phenoxyphenol (5). The remarkable observation that replacement of the ring A chlorine on 2-phenoxyphenol resulted in the reappearance of slow, tight-binding inhibition, and a 450 000-fold increase in affinity, indicated that the presence of a substituent at this position was critical for binding. To probe this effect in more detail, we extended our SAR study to include two analogues in which the ring A chlorine atom had been replaced with a fluorine (**4**) or a methyl (**5**) substituent.

Both analogues **4** and **5** are slow, tight-binding inhibitors of FabI, thus confirming that a substituent at the 5-position on ring A is critical for the slow binding step observed in the inhibition of FabI by the phenoxyphenols. However, the affinity of both these analogues for FabI is significantly reduced compared to analogue **3** and triclosan. Replacement of the chlorine in **3** with a fluorine (**4**) reduces the affinity of the inhibitor for the E·NAD^+ FabI complex 3000-fold. In addition, binding of **4** to the E·NADH form of the enzyme can now also be observed, albeit 10- to 100-fold less tightly than to the oxidized cofactor complex. While the pK_a values for **3** and **4** are similar, the van der Waals radius of fluorine is 0.5 Å smaller than that of chlorine. Thus, the reduction in analogue affinity of **4** compared to **3** is most likely due to alterations in the interaction of the ring A substituent with F203. If this effect is primarily steric in origin, then it would be predicted that analogue **5** would bind to FabI more tightly than **4**, since the van der Waals radius of the methyl substituent in **5** differs from that of chlorine by only 0.2 Å (2 and 1.8 Å, respectively). However, no interaction of **5** with the E·NAD^+ complex can be detected. Instead, **5** binds exclusively to the E·NADH form of FabI with 6000-fold lower affinity than **3** binding to the E·NAD^+ FabI complex. Since the affinities of **4** and **5** for the E·NADH FabI complex only differ by ca. 20−30-fold, the major effect

on replacing the ring A chlorine with fluorine and methyl substituents has been to drastically alter the affinity of the inhibitor for the E·NAD^+ form of FabI. In addition, both analogue **3** as well as triclosan may also bind to the E·NADH complex with nanomolar affinity. However, since these compounds bind to E·NAD^+ with picomolar affinity, then an interaction with E·NADH would be masked.

The MIC values of **4** and **5** are raised 2−3-fold compared to triclosan, indicating that these analogues, despite binding several orders of magnitude less tightly to FabI than triclosan, have similar abilities to inhibit cell growth. This could arise if the potency of each inhibitor with regard to their MICs is governed by the concentration of target in the cell. For example, if the concentration of FabI in the cell is 1 μM, then at least 1 μM analogue will be needed to completely inhibit the enzyme. At these concentrations of enzyme and inhibitor, inhibition constants of 10, 1, and 0.1 nM will give 90, 97, and 99% enzyme inhibition, respectively.

2-(2-Hydroxyphenyl)-phenol (6), 2-(2-hydroxybenzyl)-phenol (7), and 4-(4-hydroxyphenyl)-phenol (8). Analogue **6**, differing from 2-phenoxyphenol (**2**) by the addition of a 2-hydroxy group to ring B, is a classical, reversible inhibitor of the FabI enzyme and shows uncompetitive inhibition with respect to DDCoA (K_{ii} = 0.15 μM), indicating that it binds after the varied substrate. Analogue **6** therefore binds with similar affinity to FabI compared to **2**. The major difference between these two analogues is that **6** is an uncompetitive inhibitor while **2** is a noncompetitive inhibitor. Uncompetitive inhibition is assumed to result from binding only to the E·NAD^+ form of FabI while noncompetitive inhibition results from binding to both E·NAD^+ and E·NADH.[22] Thus, addition of the second hydroxyl to 2-phenoxyphenol results in an altered preference for the two cofactor-bound forms of the enzyme, a theme that runs through interaction of the ENRs with triclosan analogues.[22,30] In addition, the MIC value for **6** is 7-fold higher compared to triclosan, consistent with the reduced affinity of this analogue for FabI.

To examine the role of the bridging oxygen in FabI binding and the inhibition of cell growth, this atom was replaced by a methylene group (**7**). Previous studies have indicated that such a replacement would impair binding to the enzyme.[19] Our data show that the affinity for the enzyme is reduced more than 10^6-fold compared to triclosan and 200-fold compared to **6**. In addition the MIC is raised more than 20-fold compared to **6**. In agreement with previous studies,[12] these data clearly show that the bridging oxygen is critical for enzyme inhibition and biological activity. The substantial difference in the interaction of **7** with FabI compared to **6**, likely results primarily from removal of the hydrogen bonding interaction between the bridging oxygen and the 2′-hydroxyl group of the nicotinamide ribose ring. Finally, comparison of **6** and analogue **8**, in which the two hydroxyl groups are now para to the bridging oxygen, substantiates the requirement for an ortho hydroxyl group in the interaction of the inhibitors with FabI and in preventing cell growth.

Interaction of the Inhibitors with E·NAD^+ and E·NADH. We concluded from the inhibition of mutant FabIs by triclosan that whereas triclosan binds preferentially to the E·NAD^+ form of the wild-type enzyme, mutagenesis alters the relative affinity of triclosan for the E·NAD^+ and E·NADH forms of the enzyme.[30] This phenomenon was also observed in the inhibition of the *M. tuberculosis* ENR (InhA) by triclosan[22] and is again highlighted in the present studies. Two points can be made from the current analysis. First, alteration in the relative affinity for E·NAD^+ and E·NADH is observed for both slow, tight-binding inhibitors (**1**, **3**−**5**) and also for the classical reversible inhibitors (**2**, **6**−**8**). Consequently, whatever structural change(s) is responsible for slow-binding inhibition, it is not directly linked to whether the inhibitor binds preferentially to E·NAD^+ or E·NADH. Second, our SAR study demonstrates that subtle changes in the electronic and steric properties of ring A (**3**−**5**) have a dramatic effect on the affinity of the inhibitor for the enzyme and that these effects are dominated by alterations in affinity for E·NAD^+, while the affinity of the analogues for E·NADH remains largely unchanged. Of course, the ability to detect binding to either or both cofactor-bound forms of the enzyme is dictated by the relative affinities of the analogues for these two enzyme complexes. Thus, **3** binds only to E·NAD^+ (K_1 = 1.1 pM), **4** binds to both E·NAD^+ (K_1 = 3.2 nM) and E·NADH (K_2 = 240 nM), while **5** only binds to E·NADH (K_2 = 7.2 nM). For the interaction of **5** with E·NAD^+ to be masked by binding to E·NADH, we estimate that K_1 (binding to E·NAD^+) must be at least 2 orders of magnitude larger than the value of K_2 (7.2 nM) observed for the interaction of **5** with E·NADH. Thus, replacement of the ring A chlorine with fluorine decreases the affinity of the analogue for E·NAD^+ by 4.8 kcal/mol, while replacement with a methyl group decreases the affinity by at least 8 kcal/mol (K_1 estimated as 0.7 μM for analogue **5**).

The relative affinity of analogues **3**−**5** for the E·NAD^+ FabI complex is likely governed by modulation of the three principal interactions that exist in the complex with ring A, namely, the interaction of the 5-chloro group with F203, hydrogen bonding interactions involving the hydroxyl group and the stacking interaction between ring A and the oxidized cofactor. In an attempt to gain insight into the importance of the electrostatic interaction between the aromatic ring A and the oxidized nicotinamide ring, we performed a simple electrostatic calculation, the results of which are given in Table 2. These experiments revealed that **3** interacts more strongly with NAD^+ by 0.63 kcal/mol compared to **4**, 1 kcal/mol compared to **5** and 1.55 kcal/mol compared to **2**. While the calculated energies largely follow the observed affinities of the analogues for FabI, the differences between the experimental binding energies for E·NAD^+ vary by much larger amounts (4.8−9.4 kcal/mol; Table 2). Differences between the calculated and experimental energies will be present since the calculations do not account for changes in desolvation energies nor differences in binding mode or conformational changes in either the triclosan analogues, NAD^+ or FabI. Given these approximations, however, the computational data suggest that changes in the stacking interaction between ring A and NAD^+ resulting from differences in electron donation/withdrawal at the 5-position are small compared to the overall alteration

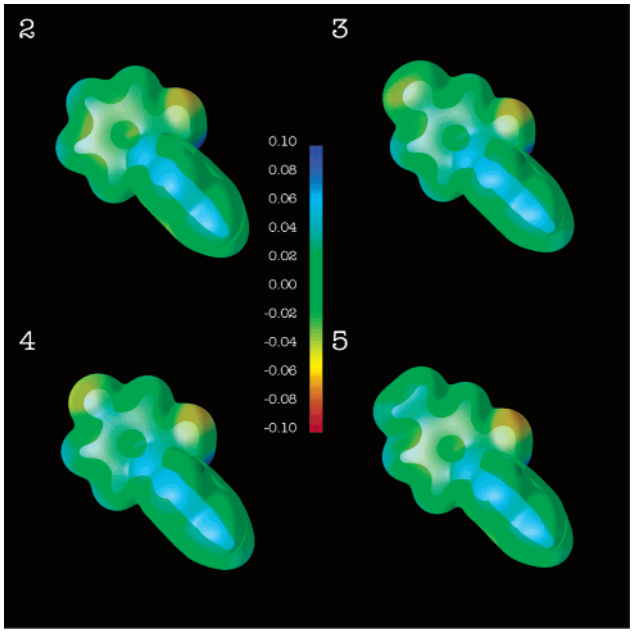

Figure 4. Visual representation of the electron density in the ring A of analogues **2**−**5**. The calculated electrostatic potential of each analogue has been mapped to its size-density surface (electron density contour value = 0.002 au). A second electron density surface (contour value = 0.1 au) is shown to facilitate differentiation of the four ligands.

in affinity of these analogues for FabI. The small changes in the calculated stacking interactions through the analogue series reflect the relatively modest changes in electron density between analogues **2**−**5**. This is shown visually in Figure 4, where the calculated electrostatic potential of each analogue has been mapped to its size-density surface. In addition, our pK_a measurements indicate that all three analogues are neutral when bound to FabI and thus the large changes in affinity through the analogue series also likely does not arise from alteration in hydrogen bonding interactions involving the ring A hydroxyl group. These data therefore suggest that the interaction of the ring A substituent with F203 is a major determinant in controlling the affinity of the analogues for the E·NAD$^+$ FabI complex. Inspection of Figure 4 supports this hypothesis, as the largest differences in electron densities are localized to the 5 substituent itself. Further insight into the interaction of the triclosan analogues with FabI will be provided by a more rigorous computational analysis in which binding free energies will be calculated using free energy perturbation formalism coupled with molecular dynamics simulations of the protein−inhibitor complex.

Conclusion

The SAR of triclosan analogue inhibitors with the wild-type FabI enzyme provides valuable information, which, when coupled to the analyses of inhibitor interactions with the FabI mutants reported previously[30] and to the X-ray crystal structure data,[15] significantly advances our understanding of ENR inhibition by triclosan. Triclosan is a slow, tight-binding, reversible picomolar inhibitor of the wild-type *E. coli* FabI, binding preferentially to the E·NAD$^+$ complex. The 5-chloro substituent on ring A is crucial for tight-binding and essential for slow-binding inhibition. Removal of the

Scheme 3[a]

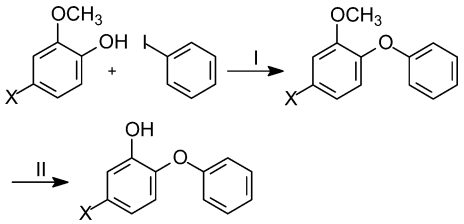

[a] Conditions: (I) Cs_2CO_3, $(CuOTf)_2$·PhH, 5 mol % EtoAc, 1-naphthoic acid, molecular sieves, toluene, 110 °C; (II) dry CH_2Cl_2, −70 °C, 1 M BBr_3, RT.

5-chloro group reduces binding 450 000-fold. In addition, subtle changes in both the steric and electronic properties of the ring A substituent have dramatic effects on affinity and the relative preference for the two cofactor-bound forms of the enzyme. The position of the ring A hydroxyl and the presence of a bridging oxygen atom are also critical for maximizing the interaction of triclosan with FabI and controlling biological activity.

Experimental Procedures

General. Triclosan (Irgasan DP 300) was a gift from Ciba Specialty Chemicals Corp (High Point, NC). Compounds **6**−**8** were purchased from TCI America (Portland, OR). Solvents and reagents were used without further purification. The progress of all reactions was monitored by TLC on precoated silica gel plates (Merck Silica gel 60 F_{254}). The developed chromatograms were viewed under UV light at 254 nm. For column chromatography Merck silica gel (70−230 mesh) was used. ^{1}H and ^{13}C NMR spectra were obtained in $CDCl_3$ using Varian spectrometers at the indicated field strengths. Chemical shifts are reported as ppm relative to TMS as an internal standard. Mass spectra were obtained at the UIUC mass spectrometry facility.

Synthesis of Triclosan Analogues (2−5). The 5-substituted phenoxyphenols were prepared by coupling the appropriate 4-substituted guaiacol with iodobenzene in the presence of a copper complex[35] followed by treatment with BBr_3 at low temperatures (Scheme 3).[36]

General Methods. Procedure I. The aryl halide (7.35 mmol), phenol (14.7 mmol), Cs_2CO_3 (32.3 mmol), $(CuOTf)_2$·PhH (0.735 mmol, 5.0 mol % Cu), ethyl acetate (0.125 mmol, 5.0 mol %), 1-naphthoic acid (32.3 mmol), molecular sieves 4 Å (1.8 g), and toluene (15 mL) were added to an oven-dried 50 mL two-necked round-bottom flask sealed with a septum and purged with nitrogen. Subsequently, the flask was heated to 110 °C under nitrogen until the reaction was shown to be complete by TLC. After being cooled to RT, the reaction mixture was extracted with dichloromethane and the extract filtered and washed with 5% NaOH. The aqueous layer was then extracted with dichloromethane, and the combined organic layers were washed with brine. The organic layer was dried over $MgSO_4$ and concentrated under vacuum to give the crude 4-substituted-2-methoxy-1-phenoxybenzene product which was subsequently purified by flash chromatography on silica gel.

Procedure II. A solution of 455 mg (1.8 mmol) of boron tribromide in 1.8 mL of dichloromethane (1.0 M solution) was added to a solution of the 4-substituted-2-methoxy-1-phenoxybenzene (1.4 mmol) in 3 mL of dry dichloromethane maintained at −70 °C under nitrogen. The reaction mixture was stirred at −70 °C for 1 h and then at RT for 3 h while monitoring by TLC. Following completion, the reaction was quenched with methanol at −70 °C and concentrated under vacuum to yield an oil. A solution of this oil in dichloromethane was washed with 10% aqueous sodium bicarbonate solution, and the organic layer was separated and washed with water and then with brine. The organic layer was then dried over $MgSO_4$, concentrated under vacuum, and the crude product purified by flash chromatography on silica gel.

1-Methoxy-2-phenoxybenzene. Procedure I was used to convert 2-methoxyphenol and iodobenzene to the target product. Purification by flash chromatography (5% ethyl acetate/hexane) gave the analytically pure product as a yellow solid (4.4 g, 79%). ^{1}H NMR (250 MHz) ($CDCl_3$) δ 7.32−7.25 (m,3H), 7.10−6.88 (m,6H), 3.83 (s,3H); ^{13}C NMR (250 MHz, $CDCl_3$) δ 157.92, 151.44, 145.05, 129.46, 124.75, 122.42, 121.08, 121.05, 117.18, 112.80, 55.94; HRMS [M^+] Calculated for $C_{13}H_{12}O_2$: 200.0837; Found: 200.0836.

2-Phenoxyphenol (2). Procedure II was used to convert 1-methoxy-2-phenoxybenzene to the target product. Purification by flash chromatography (5% ethyl acetate/hexane) gave the analytically pure product as a white solid (2.6 g, 73%). ^{1}H NMR (300 MHz) ($CDCl_3$) δ 7.37−7.31 (m,2H), 7.14−7.01 (m, 5H), 6.90−6.83 (m,2H), 5.56 (s,1H); ^{13}C NMR (250 MHz, $CDCl_3$) δ 156.75, 147.48, 143.45, 129.84, 124.74, 123.56, 120.60, 118.88, 117.96, 116.18; HRMS [M^+] Calculated for $C_{12}H_{10}O_2$: 186.0681; Found: 186.0683.

4-Chloro-2-methoxy-1-phenoxybenzene. Procedure I was used to convert 4-chloro-2-methoxyphenol and iodobenzene to the target compound. Purification by flash chromatography (5% ethyl acetate/hexane) gave the analytically pure product as a white solid (2.1 g, 53%). ^{1}H NMR (250 MHz) ($CDCl_3$) δ 7.35−6.94 (m, 8H), 3.87 (s,3H); ^{13}C NMR (250 MHz, $CDCl_3$) δ 157.55, 151.88, 143.73, 129.53, 122.69, 121.66, 120.79, 118.80, 116.40, 113.33, 56.06; HRMS [M^+] Calculated for $C_{13}H_{11}ClO_2$: 234.0448; Found: 234.0443.

5-Chloro-2-phenoxyphenol (3). Procedure II was used to convert 4-chloro-2-methoxy-1-phenoxybenzene to the target compound. Purification by flash chromatography (5% ethyl acetate/hexane) gave the analytically pure product as a white solid (627 mg, 67%). ^{1}H NMR (250 MHz) ($CDCl_3$) δ 7.38−7.31 (m,2H), 7.16−7.1 (m,1H), 7.05−6.98 (m,3H), 6.80−6.79 (d,2H), 5.66 (s,1H); ^{13}C NMR (250 MHz, $CDCl_3$) δ 156.36, 148.01, 142.36, 129.98, 129.39, 123.97, 120.56, 119.39, 118.01, 116.55; HRMS [M^+] Calculated for $C_{12}H_9ClO_2$: 220.0291; Found: 220.0293.

4-Fluoro-1-phenoxy-2-methoxybenzene. Procedure I was used to convert 4-fluoro-2-methoxyphenol and iodobenzene to the target compound. Purification by flash chromatography (5% ethyl acetate/hexane) gave the analytically pure product as a white solid (1.3 g, 83%). ^{1}H NMR (250 MHz) ($CDCl_3$) δ 7.36−7.23 (m,2H), 7.12−6.87 (m,4H), 6.76−6.58 (m,2H), 3.80 (s,3H); ^{13}C NMR (250 MHz, $CDCl_3$) δ 161.73, 158.03 d, 152.48 d, 140.63 d, 129.49, 122.30, 122.06 d, 116.45, 106.80 d, 100.97, 56.08; HRMS [M^+] Calculated for $C_{13}H_{11}FO_2$: 218.0743; Found: 218.0745.

5-Fluoro-2-phenoxyphenol (4). Procedure II was used to convert 4-fluoro-1-phenoxy-2-methoxybenzene to the target compound. Purification by flash chromatography (5% ethyl acetate/hexane) gave the analytically pure product as a white solid (1.0 g, 92%). ^{1}H NMR (600 MHz) ($CDCl_3$) δ 7.35−7.32 (t,2H), 7.13−7.10 (t,1H), 6.99−6.98 (d,1H), 6.86−6.84 (m,1H), 6.80−6.78 (dd,1H), 6.58−6.54 (m.1H); 5.64 (s,1H); ^{13}C NMR (250 MHz, $CDCl_3$) δ 161.47, 157.31 d, 148.54 d, 139.39 d, 129.94, 123.61, 119.86 d, 117.42, 107.01 d, 103.89 d; HRMS [M^+] Calculated for $C_{12}H_9FO_2$: 204.0587; Found: 204.0589.

2-Methoxy-4-methyl-phenoxybenzene. Procedure I was used to convert 4-methyl-2-methoxyphenol and iodobenzene to the target compound. Purification by flash chromatography (5% ethyl acetate/hexane) gave the analytically pure product as a white solid (847 mg, 53%). ^{1}H NMR (250 MHz) ($CDCl_3$) δ 7.29−7.23 (m,2H), 7.03−6.71 (m,6H), 3.80 (s,3H), 2.35 (s,3H); ^{13}C NMR (250 MHz, $CDCl_3$) δ 158.33, 151.23, 142.43, 134.84, 129.39, 122.08, 121.42,121.21, 116.72, 113.73, 55.91, 21.29; HRMS [M^+] Calculated for $C_{14}H_{14}O_2$: 214.0994; Found: 214.0997.

5-Methyl-2-phenoxyphenol (5). Procedure II was used to convert 2-methoxy-4-methyl-phenoxybenzene to the target compound. Purification by flash chromatography (5% ethyl acetate/hexane) gave the analytically pure product as white solid (600 mg, 71%). ^{1}H NMR (600 MHz) ($CDCl_3$) δ 7.34−7.30 (t,2H), 7.10−7.09 (t,1H), 7.00−6.99 (d,2H), 6.87 (s,1H), 6.80−6.78 (d,1H), 6.66−6.64 (d,1H), 5.43 (s,1H), 2.31 (s,3H); ^{13}C NMR (250 MHz, $CDCl_3$) δ 157.16, 147.22, 140.74, 134.91, 129.71, 123.15, 121.08, 119.09, 117.37, 116.69; HRMS [M^+] Calculated for $C_{13}H_{12}O_2$: 200.0837; Found: 200.0835.

Preparation of Triclosan and Triclosan Analogue Solutions. Triclosan and analogues were added to the final concentrations indicated from serially diluted stock solutions in Me_2SO. The Me_2SO concentration in all the assays was maintained at 0.5%. Control experiments demonstrated that this concentration of Me_2SO did not affect FabI activity.

Substrates and Enzymes. *trans*-2-Dodecenoyl-coenzyme A (DDCoA) was synthesized from *trans*-2-dodecenoic acid using the mixed anhydride method as described previously.[37] Wild-type FabI was expressed and purified as described previously.[30]

Determination of Inhibition Constants for the Binding of the Triclosan Analogues to Wild-type FabI. All experiments were carried out on a Cary 100 Bio (Varian) spectrophotometer at 25 °C in 30 mM PIPES and 150 mM NaCl (pH 8.0). Kinetic parameters were determined spectrophotometrically by following the oxidation of NADH to NAD^+ at 340 (ϵ = 6.3 mM^{-1} cm^{-1}) or 370 nm (ϵ = 2.4 mM^{-1} cm^{-1}).

Slow, Tight-Binding Inhibitors. The inhibition of FabI by analogues **3**, **4**, and **5** was performed using the procedure developed by Ward et al.[13] and previously used to quantitate the binding of triclosan to wild-type and mutant FabIs.[30] This method was developed since triclosan is a slow, tight-binding inhibitor of FabI and interacts specifically with the E·NAD^+ form of the enzyme. Consequently, since formation of the enzyme−inhibitor complex occurs slowly with respect to substrate reduction and since triclosan binds preferentially to an enzyme−product complex, typical progress curve analysis of slow, tight-binding inhibition cannot be used to analyze inhibitor binding. Instead, the enzyme was preincubated with triclosan and NAD^+ in the presence of saturating NADH so that only a small fraction of the enzyme was in the E·NAD^+ form, thus reducing the affinity of triclosan to measurable levels.[13,30] Following this protocol, wild-type FabI (7 nM) was preincubated in the presence of a fixed concentration of NAD^+ at an NADH concentration of 250 μM and with varying concentrations of analogue (0, 0.03, 0.08, 0.1, 0.15, and 0.2 μM) for 5 h at 4 °C. The mixture was warmed to room temperature and the assay was initiated by the addition of DDCoA (80 μM). The initial velocity obtained, which was proportional to the amount of active enzyme present in the assay, was fitted to eq 1, where v_0 was the rate in the absence of inhibitor and [I] was the inhibitor concentration, to generate an apparent inhibition constant K_i'.

$$v = v_0/(1 + [I]/K_i') \quad (1)$$

The K_i' determinations were repeated at different concentrations of NAD^+ (7.4−200 μM) to generate a series of K_i' values as a function of NAD^+. For analogues **4** and **5**, a series of K_i' values determined as a function of NADH were also obtained by repeating the inhibition experiments at a fixed concentration of NAD^+ (50 μM) and varying the NADH concentration from 6.8 μM to 1 mM (**4**) or from 6.8 to 350 μM (**5**). Subsequently, the dependence of K_i' on the concentration of the varied cofactor is analyzed using eq 2.

$$K_i' = (1 + [NADH]/K_{dNADH} + [NAD^+]/K_{dNAD})/(([NADH]/(K_{dNADH}K_2)) + ([NAD^+]/(K_{dNAD}K_1))) \quad (2)$$

K_1 and K_2 in eq 2 are defined in Scheme 2 and represent the inhibition constant for inhibitor binding to the E·NAD^+ and E·NADH forms of the enzyme, respectively. K_{dNADH} and K_{dNAD} are the dissociation constants for NADH and NAD^+ binding to free enzyme, respectively. A value of 5.6 μM was used for K_{dNADH},[13] while a value of 1.1 mM was used for K_{dNAD}.[30]

Equation 2 represents the general case in which the inhibitor binds to both cofactor-bound forms of the enzyme. For the triclosan analogues in which data fitting returned a large (>1 M) value for K_2, it was concluded that the inhibitor bound to E·NAD^+ but not to E·NADH, and vice versa when fitting gave K_1 > 1 M. In such cases, to confirm that binding

to a particular cofactor-bound form of the enzyme was negligible, data were reanalyzed using eqs 3 or 4, which assume binding of inhibitor to only the E·NAD^+ or E·NADH forms of the enzyme, respectively.

Inhibitor binds only to E·NAD^+:

$$K_i' = (1 + [NADH]/K_{dNADH} + [NAD^+]/K_{dNAD})/([NAD^+]/(K_{dNAD}K_1)) \quad (3)$$

Inhibitor binds only to E·NADH:

$$K_i' = (1 + [NADH]/K_{dNADH} + [NAD^+]/K_{dNAD})/([NADH]/(K_{dNADH}K_2)) \quad (4)$$

In all of these cases, the fit to eqs 3 or 4 was comparable to that found for eq 2 and returned essentially the same values for the remaining variables.

Steady-State Inhibition Studies. For analogues **2** and **6**−**8**, initial inhibition experiments demonstrated that these compounds were not slow, tight-binding inhibitors. Consequently, conventional steady-state inhibition experiments were used to determine the affinity of these compounds for FabI, as well as the type of inhibition. For analogue **2** the inhibition constants were calculated by determining k_{cat} and K_{mDDCOA} at a fixed, saturating concentration of NADH (250 μM) and by varying the concentration of DDCoA (2.5−50 μM) and **2** (0, 0.26, 0.9 μM). For analogues **6**−**8**, the inhibition constants were determined in the same manner. Analogue concentrations used were as follows: **6** (0, 0.1, 0.35 and 0.75 μM); **7** (0, 7, 14, and 70 μM); **8** (0, 484, 1635, 2920 μM). Each initial velocity was determined in duplicate and at least five different DDCoA concentrations were examined. Initial velocity data obtained at various substrate concentrations in the presence of varying amounts of an analogue were initially analyzed by plotting *v* versus *v*/[S], to determine whether the inhibition was competitive, uncompetitive, or noncompetitive with respect to the varied substrate. For analogues **2**, **7**, and **8** the *v* versus *v*/[S] plots indicated noncompetitive inhibition in which the inhibitor binds both before and after the varied substrate. Consequently, the data were analyzed using eq 5, where [S] is the concentration of the varied substrate, [I] is the concentration of the inhibitor, *V* is the maximum velocity, and K_m is the Michaelis−Menten constant. By convention, K_{is} and K_{ii} in eq 5 are the dissociation constants for binding of the inhibitor to the enzyme before and after the varied substrate, respectively. For analogue **6**, the *v* versus v/[S] plot indicated uncompetitive inhibition in which the inhibitor binds after the varied substrate, and the experimental data were analyzed using eq 6, where the parameters have the same meaning as above.

$$v_i = (V([S]/K_m))/(1 + [I]/K_{is} + [S]/K_m + ([S][I]/K_{ii} + K_m)) \quad (5)$$

$$v_i = (V[S]/([I]/K_{ii}))/([S] + K_m/(1 + [I]/K_{ii})) \quad (6)$$

Determination of pK_a Values for Triclosan and Analogues 2−5. To determine the effect that binding has on the electronic properties of the compounds, the pK_a of triclosan and analogues **2**−**5** were determined by the measurement of the UV−vis absorbance of the conjugate base in several buffer solutions at different pH values ranging from pH 6.8 to pH 10.8. Stock solutions of the compounds were made in DMSO and diluted into buffer solutions such that the concentration of DMSO was maintained at 0.4−0.5%. The absorbance values were used to determine the concentration of the A^- form and a plot of fraction of the [A^-] versus pH yielded the pK_a value. To determine the pK_a of triclosan bound to FabI, UV−visible absorption spectra were acquired at various pH values (6.1−9.3) of solutions containing 18 μM FabI, 54 μM NAD^+, and 18 μM triclosan that had been incubated for 5 h. Spectra of triclosan bound to FabI were obtained by first subtracting a spectrum of FabI and NAD^+ from that of the ternary complex and then interactively subtracting the spectrum of neutral triclosan to provide the spectrum of the ionized inhibitor. Buffer solutions used were (pH 6.0−8.0), 30 mM PIPES, 150 mM NaCl; (pH 8.2−8.8), 30 mM Tris.HCl, 150 mM NaCl; (pH 9.0−10.0), 30 mM K_2CO_3, 150 mM NaCl.

Calculated Interaction Energies Between Analogues 1−5 and NAD^+. The interaction between triclosan analogues **1**−**5** and NAD^+ was calculated with a molecular mechanics approach using the AMBER 7 modeling package and the parm99 force field. The gas phase electron density and electrostatic potential of each analogue was calculated quantum mechanically with Gaussian 98 (HF/6-31G*). The partial charges of each analogue were derived by a two-stage fitting procedure (RESP) to the quantum mechanically calculated electrostatic potential. All analogues were assumed to adopt the same conformation and binding mode as observed in FabI/NAD^+ and triclosan tertiary complex. Each analogue was subjected to local energy minimization with positional restraints on all atoms except the modified substituents. The net interaction between analogues and NAD+, including van der Waals and electrostatic energies, was then calculated without constraints.

Determination of Whole Cell Antimicrobial Activity. Whole-cell antimicrobial activity was determined by a broth microdilution procedure. Stock solutions of triclosan and analogues **2**−**5** were made in 1 M KOH. These solutions were serially diluted into 50 mM Na_2CO_3 pH 8.5 buffer. The stock solutions were serially diluted into cation-adjusted Mueller-Hinton broth (Becton Dickenson, Cockeysville, MD) on a 96-well microtiter plate. After dilution, 20 μL of *E. coli* (BL21 (DE3) pLysS) cells was added to each well of the microtiter plate. The final test concentrations ranged from 0.01 to 64 μg/mL. Inoculated plates were incubated at 37 °C for 24h. The minimum inhibitory concentration (MIC) was determined as the lowest concentration of compound that inhibited visible growth as estimated by OD_{600} readings using a 96-well plate reader.

Acknowledgment. High resolution mass spectra were obtained in the Mass Spectrometry Laboratory, School of Chemical Sciences, University of Illinois, supported in part by a grant from the National Institute of General Medical Sciences (GM 27029). The authors thank Dr. Adrian Whitty and Prof. Liz Hedstrom for helpful discussions.

Appendix

Abbreviations: FAS, fatty acid biosynthesis; KAS, β-ketoacyl-ACP synthase; TLM, thiolactomycin; CER, cerulenin; ENR, enoyl reductase; InhA, the enoyl reductase from *Mycobacterium tuberculosis*; FabI, the enoyl reductase from *Escherichia coli*; KasA, the β-ketoacyl-ACP synthase from *M. tuberculosis*; CoA, coenzyme A (lithium salt); DDCoA, *trans*-2-dodecenoyl-CoA.

References

(1) Heath, R. J.; White, S. W.; Rock, C. O. Lipid biosynthesis as a target for antibacterial agents. *Prog. Lipid Res.* **2001**, *40*, 467−497.
(2) Rock, C. O.; Cronan, J. E. *Escherichia coli* as a model for the regulation of dissociable (type II) fatty acid biosynthesis. *Biochim. Biophys. Acta* **1996**, *1302*, 1−16.
(3) Campbell, J. W.; Cronan, J. E., Jr. Bacterial fatty acid biosynthesis: targets for antibacterial drug discovery. *Annu. Rev. Microbiol.* **2001**, *55*, 305−332.
(4) Seefeld, M. A.; Miller, W. H.; Newlander, K. A.; Burgess, W. J.; Payne, D. J. et al. Inhibitors of bacterial enoyl acyl carrier protein reductase (FabI): 2,9-disubstituted 1,2,3,4-tetrahydropyrido[3,4-b]indoles as potential antibacterial agents. *Bioorg. Med. Chem. Lett.* **2001**, *11*, 2241−2244.
(5) Heerding, D. A.; Chan, G.; DeWolf, W. E.; Fosberry, A. P.; Janson, C. A. et al. 1,4-Disubstituted imidazoles are potential antibacterial agents functioning as inhibitors of enoyl acyl carrier protein reductase (FabI). *Bioorg. Med. Chem. Lett.* **2001**, *11*, 2061−2065.

(6) Miller, W. H.; Seefeld, M. A.; Newlander, K. A.; Uzinskas, I. N.; Burgess, W. J. et al. Discovery of aminopyridine-based inhibitors of bacterial enoyl-ACP reductase (FabI). *J. Med. Chem.* **2002**, *45*, 3246−3356.
(7) Payne, D. J.; Miller, W. H.; Berry, V.; Brosky, J.; Burgess, W. J. et al. Discovery of a novel and potent class of FabI-directed antibacterial agents. *Antimicrob. Agents Chemother.* **2002**, *46*, 3118−3124.
(8) Schweizer, H. P. Triclosan: a widely used biocide and its link to antibiotics. *FEMS Microbiol. Lett.* **2001**, *202*, 1−7.
(9) Regos, J.; Zak, O.; Solf, R.; Vischer, W. A.; Weirich, E. G. Antimicrobial spectrum of triclosan, a broad-spectrum antimicrobial agent for topical application. II. Comparison with some other antimicrobial agents. *Dermatologica* **1979**, *158*, 72−79.
(10) Vischer, W. A.; Regos, J. Antimicrobial spectrum of Triclosan, a broad-spectrum antimicrobial agent for topical application. *Zentralbl. Bakteriol. [Orig A]* **1974**, *226*, 376−389.
(11) McMurry, L. M.; Oethinger, M.; Levy, S. B. Triclosan targets lipid synthesis. *Nature* **1998**, *394*, 531−532.
(12) Heath, R. J.; Yu, Y. T.; Shapiro, M. A.; Olson, E.; Rock, C. O. Broad spectrum antimicrobial biocides target the FabI component of fatty acid synthesis. *J. Biol. Chem.* **1998**, *273*, 30316−30320.
(13) Ward, W. H.; Holdgate, G. A.; Rowsell, S.; McLean, E. G.; Pauptit, R. A.; Clayton, E.; Nichols, W. W.; Colls, J. G.; Minshull, C. A.; Jude, D. A.; Mistry, A.; Timms, D.; Camble, R.; Hales, N. J.; Britton, C. J.; Taylor, I. W. Kinetic and structural characteristics of the inhibition of enoyl (acyl carrier protein) reductase by triclosan. *Biochemistry* **1999**, *38*, 12514−12525.
(14) Levy, C. W.; Roujeinikova, A.; Sedelnikova, S.; Baker, P. J.; Stuitje, A. R. et al. Molecular basis of triclosan activity. *Nature* **1999**, *398*, 383−384.
(15) Stewart, M. J.; Parikh, S.; Xiao, G.; Tonge, P. J.; Kisker, C. Structural basis and mechanism of enoyl reductase inhibition by triclosan. *J. Mol. Biol.* **1999**, *290*, 859−865.
(16) Roujeinikova, A.; Levy, C. W.; Rowsell, S.; Sedelnikova, S.; Baker, P. J.; Minshull, C. A.; Mistry, A.; Colls, J. G.; Camble, R.; Stuitje, A. R.; Slabas, A. R.; Rafferty, J. B.; Pauptit, R. A.; Viner, R.; Rice, D. W. Crystallographic analysis of triclosan bound to enoyl reductase. *J. Mol. Biol.* **1999**, *294*, 527−535.
(17) Heath, R. J.; Rock, C. O. A triclosan-resistant bacterial enzyme. *Nature* **2000**, *406*, 145−146.
(18) Heath, R. J.; Su, N.; Murphy, C. K.; Rock, C. O. The enoyl-[acyl-carrier-protein] reductases FabI and FabL from *Bacillus subtilis*. *J. Biol. Chem.* **2000**, *275*, 40128−40133.
(19) Heath, R. J.; Li, J.; Roland, G. E.; Rock, C. O. Inhibition of the Staphylococcus aureus NADPH-dependent enoyl-acyl carrier protein reductase by triclosan and hexachlorophene. *J. Biol. Chem.* **2000**, *275*, 4654−4659.
(20) Marcinkeviciene, J.; Jiang, W.; Kopcho, L. M.; Locke, G.; Luo, Y. et al. Enoyl-ACP reductase (FabI) of Haemophilus influenzae: steady-state kinetic mechanism and inhibition by triclosan and hexachlorophene. *Arch. Biochem. Biophys.* **2001**, *390*, 101−108.
(21) McMurry, L. M.; McDermott, P. F.; Levy, S. B. Genetic evidence that InhA of *Mycobacterium smegmatis* is a target for triclosan. *Antimicrob. Agents Chemother.* **1999**, *43*, 711−713.
(22) Parikh, S. L.; Xiao, G.; Tonge, P. J. Inhibition of InhA, the enoyl reductase from *Mycobacterium tuberculosis*, by triclosan and isoniazid. *Biochemistry* **2000**, *39*, 7645−7650.
(23) Kuo, M. R.; Morbidoni, H. R.; Alland, D.; Sneddon, S. F.; Gourlie, B. B. et al. Targeting tuberculosis and malaria through inhibition of Enoyl reductase: compound activity and structural data. *J. Biol. Chem.* **2003**, *278*, 20851−20859.
(24) Surolia, N.; Surolia, A. Triclosan offers protection against blood stages of malaria by inhibiting enoyl-ACP reductase of Plasmodium falciparum. *Nat. Med.* **2001**, *7*, 167−173.
(25) Kapoor, M.; Dar, M. J.; Surolia, N.; Surolia, A. Kinetic determinants of the interaction of enoyl-ACP reductase from Plasmodium falciparum with its substrates and inhibitors. *Biochem. Biophys. Res. Commun.* **2001**, *289*, 832−837.
(26) Perozzo, R.; Kuo, M.; bir Singh Sidhu, A.; Valiyaveettil, J. T.; Bittman, R.; Jacobs, W. R., Jr.; Fidock, D. A.; Sacchettini, J. C. Structural elucidation of the specificity of the antibacterial agent triclosan for malarial enoyl ACP reductase. *J. Biol. Chem.* **2002**, *277*, 13106.
(27) Liu, B.; Wang, Y.; Fillgrove, K. L.; Anderson, V. E. Triclosan inhibits enoyl-reductase of type I fatty acid synthase in vitro and is cytotoxic to MCF-7 and SKBr-3 breast cancer cells. *Cancer Chemother. Pharmacol.* **2002**, *49*, 187−193.
(28) Heath, R. J.; Rubin, J. R.; Holland, D. R.; Zhang, E.; Snow, M. E. et al. Mechanism of triclosan inhibition of bacterial fatty acid synthesis. *J. Biol. Chem.* **1999**, *274*, 11110−11114.
(29) Qiu, X.; Janson, C. A.; Court, R. I.; Smyth, M. G.; Payne, D. J. et al. Molecular basis for triclosan activity involves a flipping loop in the active site. *Protein Sci.* **1999**, *8*, 2529−2532.
(30) Sivaraman, S.; Zwahlen, J.; Bell, A. F.; Hedstrom, L.; Tonge, P. J. Structure−Activity Studies of the Inhibition of FabI, the Enoyl Reductase from *Escherichia coli*, by Triclosan: Kinetic Analysis of Mutant FabIs. *Biochemistry* **2003**, *42*, 4406−4413.
(31) Morrison, J. F.; Walsh, C. T. The behavior and significance of slow-binding enzyme inhibitors. *Adv. Enzymol.* **1988**, *61*, 201−301.
(32) Baldock, C.; Rafferty, J. B.; Sedelnikova, S. E.; Baker, P. J.; Stuitje, A. R.; Slabas, A. R. A mechanism of drug action revealed by structural studies of enoyl reductase. *Science* **1996**, *274*, 2107−2110.
(33) Levy, C. W.; Baldock, C.; Wallace, A. J.; Sedelnikova, S.; Viner, R. C.; Clough, J. M.; Stuitje, A. R.; Slabas, A. R.; Rice, D. W.; Rafferty, J. B. A study of the structure−activity relationship for diazaborine inhibition of *Escherichia coli* enoyl-ACP reductase. *J. Mol. Biol.* **2001**, *309*, 171−180.
(34) Roujeinikova, A.; Sedelnikova, S.; de Boer, G. J.; Stuitje, A. R.; Slabas, A. R.; Rafferty, J. B.; Rice, D. W. Inhibitor binding studies on enoyl reductase reveal conformational changes related to substrate recognition. *J. Biol. Chem.* **1999**, *274*, 30811−30817.
(35) Marcoux, J.-F.; Doye, S.; Buchwald, S. L. *J. Am. Chem. Soc.* **1997**, *119*, 10539−10540.
(36) Neumeyer, J. L.; Baindur, N.; Yuan, J.; Booth, G.; Seeman, P. et al. Development of a high affinity and stereoselective photoaffinity label for the D-1 dopamine receptor: synthesis and resolution of 7-[125I]iodo-8-hydroxy-3-methyl-1-(4′-azidophenyl)-2,3,4,5-tetrahydro- 1H-3-benzazepine. *J. Med. Chem.* **1990**, *33*, 521−526.
(37) Parikh, S.; Moynihan, D. P.; Xiao, G.; Tonge, P. J. Roles of tyrosine 158 and lysine 165 in the catalytic mechanism of InhA, the enoyl-ACP reductase from *Mycobacterium tuberculosis*. *Biochemistry* **1999**, *38*, 13623−13634.

JM030182I